CrossMark

Field Observations of Canopy Flows over Complex Terrain

**Eleanor R. Grant · Andrew N. Ross ·
Barry A. Gardiner · Stephen D. Mobbs**

Abstract The investigation of airflow over and within forests in complex terrain has been, until recently, limited to a handful of modelling and laboratory studies. Here, we present an observational dataset of airflow measurements inside and above a forest situated on a ridge on the Isle of Arran, Scotland. The spatial coverage of the observations all the way across the ridge makes this a unique dataset. Two case studies of across-ridge flow under near-neutral conditions are presented and compared with recent idealized two-dimensional modelling studies. Changes in the canopy profiles of both mean wind and turbulent quantities across the ridge are broadly consistent with these idealized studies. Flow separation over the lee slope is seen as a ubiquitous feature of the flow. The three-dimensional nature of the terrain and the heterogeneous forest canopy does however lead to significant variations in the flow separation across the ridge, particularly over the less steep western slope. Furthermore, strong directional shear with height in regions of flow separation has a significant impact

E. R. Grant · A. N. Ross (✉)
School of Earth and Environment, Institute for Climate and Atmospheric Science,
University of Leeds, Leeds LS2 9JT, UK
e-mail: a.n.ross@leeds.ac.uk

Present address
E. R. Grant
British Antarctic Survey, High Cross, Madingley Road, Cambridge CB3 0ET, UK

B. A. Gardiner
Forest Research, Northern Research Station, Roslin, Midlothian EH25 9SY, Scotland, UK

Present address
B. A. Gardiner
INRA, UMR 1391 ISPA, 33140 Villenave D'Ornon, France

B. A. Gardiner
Bordeaux Sciences Agro, UMR 1391 ISPA, 33170 Gradignan, France

S. D. Mobbs
National Centre for Atmospheric Science and School of Earth and Environment,
University of Leeds, Leeds LS2 9JT, UK

on the Reynolds stress terms and other turbulent statistics. Also observed is a decrease in the variability of the wind speed over the summit and lee slope, which has not been seen in previous studies. This dataset should provide a valuable resource for validating models of canopy flow over real, complex terrain.

1 Introduction

In recent years there has been a growing interest in the interaction of airflow within and above forest canopies, particularly over complex terrain. This has been motivated by a number of factors. For example, the uptake of carbon dioxide by forests is an important and uncertain part of the carbon cycle. There has been a large worldwide investment in continuous measurements of the surface–atmosphere exchange of carbon dioxide (Baldocchi et al. 2001) but interpretation of these measurements requires a thorough understanding of canopy flows over complex terrain (Finnigan 2008; Belcher et al. 2008; Ross 2011). Wind damage in hilly terrain is a serious threat to managed forests (Quine and Gardiner 2007; Gardiner et al. 2013) and reduces the yield of recoverable timber, increases the cost of harvesting, decreases the landscape quality and harms established wildlife habitats (Gardiner et al. 2010; Hanewinkel et al. 2013). There is, to date, little theoretical framework for describing and understanding the turbulence structure within canopies on complex terrain, and yet this is crucial for predicting wind damage to forests. Hills and mountains exert an important drag on the atmosphere and this requires the correct parametrization in global weather and climate models (Webster et al. 2003) but the presence of a forest canopy can modify this drag (Ross and Vosper 2005). Lastly, the large worldwide investment in wind energy has wind turbines sited in forested areas of mixed topography. It is therefore essential that the yield of these turbines is quantitatively understood (Ayotte et al. 2001).

Airflow through forest canopies has been extensively studied for the last six decades, but the majority of these studies have been restricted to idealized conditions, i.e. homogeneous canopy, flat terrain, neutral to slightly unstable conditions (see e.g. Kaimal and Finnigan 1994; Finnigan 2000). Most real forests are not homogeneous and are rarely on completely flat sites and so there is a fundamental need to increase our understanding of these heterogeneous canopy flows. While there is a considerable body of literature on flows over rough hills (Kaimal and Finnigan 1994; Belcher and Hunt 1998), it is only relatively recently that much attention has been paid to canopy covered hills. This, to a large part, follows from the theoretical work of Finnigan and Belcher (2004). In addition increasing attention has been paid to heterogeneous canopy cover over the last 10 years, but again this has been largely focused on sharp forest-edge transitions (e.g. Irvine et al. 1997; Morse et al. 2002; Dupont and Brunet 2008; Romniger and Nepf 2011).

Over the last twenty years there have only been a handful of observational studies of flow over forested complex terrain, the majority of which have been limited to wind-tunnel experiments, including Ruck and Adams (1991) and Neff and Meroney (1998). Both studies investigated flow over modelled ridges covered with plant canopies of differing heights. The wind-tunnel study of Finnigan and Brunet (1995) conducted on a ridge covered with a tall canopy provided more comprehensive measurements, showing that the inflection point at the top of the canopy profile is heavily influenced by the presence of the hill. On the windward slope the inflection point was observed to disappear while on the crest of the

hill the strength of the inflection point was substantially greater. More recently a series of flume investigations (Poggi and Katul 2007a, b) explored the role of the hill-induced pressure perturbation and advection on the flow velocity. Field experiments that have measured the airflow at complex forested sites (e.g. Bradley 1980; Zeri et al. 2010) have tended to make measurements at a single tower and hence do not quantify the spatial variations in flow across the terrain.

In addition to these observations there are a number of theoretical and modelling studies, almost all of which make use of idealized terrain and a homogeneous, uniform canopy. Finnigan and Belcher (2004) extended the existing theory of Hunt et al. (1988) for flow over rough hills and developed an analytical model for flow over canopy covered hills. This model restricts itself to a shallow hill with a dense canopy (all the momentum is absorbed by drag on the foliage) but it has clearly defined the important parameters of the problem and offers a theoretical framework with which to understand the earlier wind-tunnel results. Brown et al. (2001) and Allen and Brown (2002) conducted large-eddy simulations (LES) and mixing length simulations of wind-tunnel observations using both a roughness length parametrization and a canopy model. The canopy simulations modelled the observations with better accuracy, showing reduced acceleration over the hill and an increase in the drag. Ross and Vosper (2005) conducted a series of numerical simulations comparing the use of an explicit canopy model with a roughness length parametrization. Results from both roughness length and canopy simulations are compared to the observational data of Finnigan and Brunet (1995), demonstrating the benefits of using a canopy model over a roughness length parametrization. In the last few years three more notable LES models have been developed. Dupont et al. (2008) analyze and validate results from a nested LES using the wind-tunnel results of Finnigan and Brunet (1995); Ross (2008) conducted LES of the flow over a series of small forested ridges; and Patton and Katul (2009) used LES to explore the impact of vegetation density on the flow interactions above and within vegetation on a series of gentle ridges. Other modelling studies have looked at the impact of these canopy flows on tracer transport (Ross 2011) and have begun to explore the potential impact of non-homogeneous canopies over hills (Ross and Baker 2013). To date all of these theoretical and modelling studies have focused on simple idealized terrain and, with the exception of Ross and Baker (2013), also assume a uniform homogeneous canopy.

Thanks to the combined efforts of these studies we are now able to identify and explain the key features of canopy flows over complex terrain, at least for a uniform homogeneous canopy. However, there remain few studies over more complex and realistic terrain with heterogeneous canopy cover. As has been pointed out previously (e.g. Poggi and Katul 2007a; Belcher et al. 2008), further progress has been restricted due to a lack of the field measurements necessary to validate model developments. This paper presents a unique observational dataset of airflow measurements from within and above a forest situated on a ridge and compares the results to recent idealized theoretical studies. It is the first dataset of its kind and should help to progress our understanding of this subject. Section 2 gives an overview of the field experiment and the data collected, and Sect. 3 presents results from two particular case studies of flow across the ridge under near-neutral conditions, concentrating on the mean flow and the occurrence of flow separation. Section 4 provides details of profiles of various turbulence statistics from the towers, while Sect. 5 discusses the results from this real, complex and heterogeneous field site in the context of previous idealized models of neutral flow over two-dimensional ridges covered with a uniform canopy. Results are also compared with previous observations within and above flat, homogeneous forest canopies in order to highlight the impact of the complex terrain on flow turbulence characteristics. Finally, Sect. 6 draws conclusions.

2 Overview of the Field Measurements

The field measurements were made on a forested ridge, Leac Gharbh (55°40.2′N, 5°33.6′W), located on the north-east coast of the Isle of Arran, 22 km off the south-west coast of the Scottish mainland. The island has previously been used for field measurements of boundary-layer flow and flow separation over unforested hills (Vosper et al. 2002). Typical hill heights at the northern end of Arran are between 400 and 800 m with the island's highest hill, Goat Fell (874 m), lying 6 km to the south-west of the field site. Leac Gharbh itself varies in height from approximately 160 m at the south-east to 260 m at the north-west and is 1.5 km in length (Fig. 1). The north-eastern slope of Leac Gharbh is steeper than the south-western slope (average values of H/L are 0.36 and 0.24 respectively where H is the ridge height and L is the half width of the hill) but the terrain on both slopes is inconsistent and there are areas that are both significantly shallower and significantly steeper than these values. However, on average, both slopes are well above the typical values of 0.05–0.1 required for flow separation in a canopy (Ross and Vosper 2005; Poggi and Katul 2007b). The summit of the ridge is approximately 250 m wide. The ridge is forested primarily with a dense (1600 trees per hectare) Sitka spruce (*Picea sitchensis* Bong. Carr.) plantation with an average tree height of $h = 17.5$ m. There are also patches of western hemlock (*Tsuga heterophylla*) and silver birch (*Betula pendula*) mixed in with the Sitka spruce, particularly on the north-east slope. To the southern end of the ridge there are also hybrid larch (*Larix x marschlinsii (Syn. L. x eurolepis)*) of a similar height to the Sitka spruce. Further north along the ridge and beyond the forest the land cover is rough moorland. A detailed analysis of the forest canopy was conducted by the Forestry Commission, with the survey splitting the site into 23×0.01 ha plots (Fig. 1), and for each plot the number, species and diameter at breast height (1.3 m above ground) of each tree was recorded. The height of the tree with the greatest diameter was also recorded. As the aerial photograph in Fig. 1 shows the density of the canopy varies significantly over the field site and there are several large clearings, the largest of which is 5h across (Fig. 2).

Measurements were made continually from 13 March to 14 May 2007. Three vertical profile towers (T1, T2, T3) were located across the ridge, and were supplemented with a network of 12 automatic weather stations (AWS) giving measurements near the surface (2 m above the ground). The AWS sites are labelled ARA through to ARQ and the location of each site is shown in Fig. 1. Four three-dimensional sonic anemometers sampling at 10 Hz were mounted on each tower along with six thermistor temperature sensors and six cup anemometers at various heights between 2 and 23 m. The sonic anemometers were logged using a Moxa UC-7420 low power computer at each tower running custom logging software. One-minute average values from the cup anemometers and thermistors were logged with a Campbell CR1000 data logger at each tower. Each AWS measured wind speed and wind direction at 2 m (with a wind cup and vane), temperature (with a thermistor and with a Sensiron SHT1x digital sensor) and pressure. The AWS logged data every 3 s using a custom made lower power data logger. Table 1 provides a detailed overview of the instruments used. All instrumentation was deployed within an area of less than 2 km^2. The vertical profile towers were constructed in a transect over the ridge (henceforth, the canopy transect), with Fig. 1 showing the location of each tower and AWS site. The majority of the AWS were erected in the same transect as the profile towers to provide as much information as possible over this specific area. A second, smaller transect was constructed well outside the forest ridge canopy using three AWS (henceforth the northern transect), and at each site a differential GPS survey was conducted to calculate altitude accurately. Tables 2 and 3 summarize the main features of each instrument site.
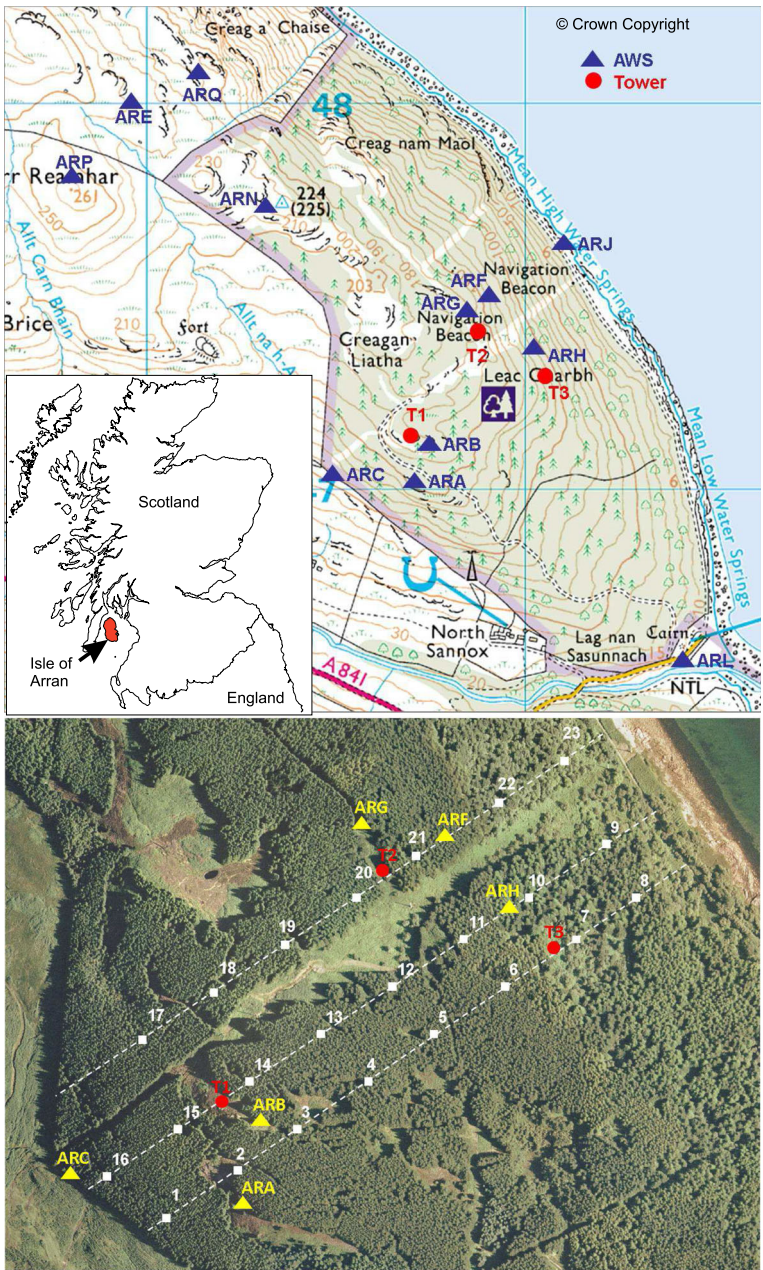
Fig. 1 *Top* 1:25000 Ordnance Survey map of the field site with instrumentation sites marked. *Red circles* indicate the vertical profile towers (T1–T3) and *blue triangles* indicate automatic weather stations (AWS). *Inset* is a map of Scotland highlighting the location of the Isle of Arran. The 1:25000 map is © Crown Copyright/database right 2010. An Ordnance Survey/EDINA supplied service. Outline map of Scotland is reproduced from Ordnance Survey map data by permission of Ordnance Survey, © Crown copyright 2013. *Bottom* Aerial photograph of the field site canopy showing the 23 canopy survey plots (*white squares*), the tower sites (*red circles*) and the AWS (*yellow triangles*). The *white squares* of the survey plots are to scale
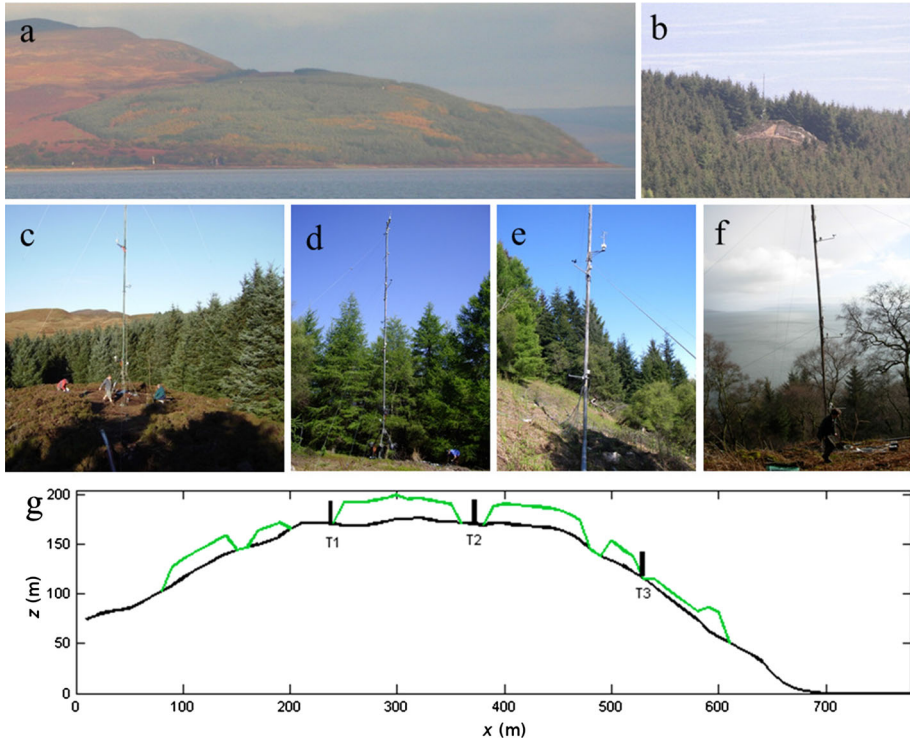
Fig. 2 Photographs from the field site showing **a** Leac Gharbh, taken from the sea looking north-west; **b** taken from AWS ARP, looking south-east, down onto T1. T1 is elevated slightly from its surroundings and is in a clearing that is approximately three canopy heights wide and five canopy heights long; **c** T1 looking north-west, showing the dense canopy to the north and east of the tower and the large clearing to the west; **d** the site at T2 looking north-east, showing the larch canopy. To the west the canopy is Sitka spruce. These two canopies are divided by a small pathway to the north-west that leads to AWS ARG; **e** T3 looking north-west, showing the dense spruce plantation upslope; **f** T3 looking east. This picture illustrates the steepness of the terrain downslope from T3. It also shows how some of the canopy (of mainly birch) directly downslope of the tower does not reach the same level as the bottom sonic anemometer, which is just visible to the right of the tower above the second cup anemometer; **g** schematic cross-section profile (west to east) of Leac Gharbh with tower locations shown and canopy marked in *green*

For the results presented here the 3-s data from the AWS were averaged. The mean wind speed is the 15-min average of the instantaneous wind speeds and the mean wind direction was determined as the direction of the averaged instantaneous wind vectors over the same period. The wind speeds presented here from the sonic anemometers are 15-min averages of the instantaneous wind speeds (for direct comparison with the cup anemometers). Wind directions are again the direction of the mean wind vector. For calculating momentum fluxes each 15-min period of data was rotated into streamwise coordinates using a double rotation (see e.g. Lee et al. 2004). The presented fluxes are therefore in streamwise coordinates, with u being in the direction of the 15-min averaged mean wind. The flux data were quality controlled using the stationarity test of Foken and Wichura (1996) with each 15-min period sub-divided into five, and a 30 % threshold for the differences to be classified as non-stationary. At the more exposed sites this resulted in less than 1 % of the data being rejected, but at some of the more sheltered in-canopy sites up to 10 % of the data was rejected. Following data

Table 1 Overview of instruments used throughout the field campaign

Instrument make and model	Use	Accuracies
3-D sonic anemometer: Metek USA-1	Four on towers T1 and T3, two at lower heights on tower T2	At $1\,\mathrm{m\,s^{-1}}$: $\pm0.1\,\mathrm{m\,s^{-1}}$ and $\pm5°$ At $4\,\mathrm{m\,s^{-1}}$: $\pm0.15\,\mathrm{m\,s^{-1}}$ and $\pm3°$. At $10\,\mathrm{m\,s^{-1}}$: $\pm0.3\,\mathrm{m\,s^{-1}}$ and $\pm2°$. For $20-50\,\mathrm{m\,s^{-1}}$: $\pm2\,\%$ and $\pm2°*$
3-D sonic anemometer: Gill R3A	Two at upper heights on T2	Wind speed: $<1\,\%$ rms, wind direction: $<\pm1\,\%$ rms**
Cup anemometer: NRG Type 40	Towers and AWS	$0.1\,\mathrm{m\,s^{-1}}$ within a range of $5–25\,\mathrm{m\,s^{-1}}$
Wind vane: NRG Type 200P	AWS	$1\,\%$
Temperature sensor: Betatherm Series 1 thermistor	Towers and AWS	$1\,\%$ at $25\,°\mathrm{C}$
Pressure sensor: Intersema MS5534	AWS	$\pm0.5\,$hPa at $25\,°\mathrm{C}$
Digital temperature sensor: Sensirion SHT1x	AWS	$\pm0.5\,°\mathrm{C}$

* Accuracy applies for horizontal wind speeds
** Accuracy applies for wind speed $<32\,\mathrm{m\,s^{-1}}$ and for wind incidence angles $\pm20°$ from the horizontal
rms root mean square

Table 2 Summary of the main features of each tower site describing canopy, altitude and general terrain

Tower	Within canopy	Canopy description	Altitude (m)	Site description
T1	Yes	Dense Sitka spruce plantation (16.8 m)	170 ± 10	Located on south-west facing slope in a large clearing (approximately $40\,\mathrm{m^2}$). Tower located to the north-east of the clearing. Steep rocky outcrop (approximately 5 m tall) dropping off to west of tower
T2	Yes	Dense Sitka spruce plantation (18.5 m)	165 ± 10	Located on summit of ridge in a small clearing (approximately $15\,\mathrm{m^2}$)
T3	Yes	Sitka spruce plantation upslope, mixed deciduous forest downslope (15.7 m)	110 ± 10	Located on north-east facing slope in a natural clearing, on significantly steeper terrain than T1 and T2

The heights included in the canopy description are mean canopy heights calculated from the survey plots nearest each site

quality control, continuous operation for 44 days between 1 April and 14 May 2007 provided 4224 15-min mean measurements from the majority of the AWS and vertical profile towers. Quality controlled data between 13 and 31 March 2007 are also available but these data are incomplete. The following analysis only uses data from 1 April until 14 May 2007, after bud burst on the trees. This minimizes the impact of changing leaf cover on the canopy drag, and hence the flow patterns in the patches of deciduous trees (mainly birch and larch).

The field campaign was dominated by anticyclonic conditions with anticyclones located over Arran for 24 of the 44 days. These anticyclonic periods were associated with low wind

Table 3 Summary of the main features of each AWS site describing canopy, altitude and general terrain

AWS	Within canopy	Canopy description	Altitude (m)	Site description
ARA	Yes	Dense Sitka spruce plantation (14.5 m)	150 ± 5	Located on south-west facing slope, with a large clearing to the south-west and extending east
ARB	Yes	Dense Sitka spruce plantation (17.6 m)	175 ± 5	Located approximately 30 m south-east of T1
ARC	Yes	Dense Sitka spruce plantation to the north-east (18.6 m), no canopy to the south-west	112 ± 5	Located on the south-west facing slope, at the edge of the plantation. Plantation to the north-east, open field to the south-west
ARE	No	NA	230 ± 1	Out of the canopy, approximately 200 m north-west of the plantation edge, on the north-east facing slope
ARF	Yes	Mixed canopy of Sitka spruce and hybrid larch (26.8 m)	135 ± 10	Located on the steep, north-west facing slope, directly downslope from T2, fully surrounded by canopy, though canopy less dense than further upslope
ARG	Yes	Dense Sitka spruce plantation (20.2 m)	180 ± 10	Located approximately 50 m north of T2 in a small clearing (approximately 5 m^2)
ARH	Yes	Mixed canopy of Sitka spruce and western hemlock (27.0 m)	115 ± 10	Located on the steep, north-east facing slope approximately 30 m north of T3. Fully surrounded by canopy though less dense than further upslope
ARJ	No	NA	8 ± 5	Located at the base of the ridge, on the coast, out of the canopy
ARL	No	NA	13 ± 5	Located at the base of the ridge, out of the canopy, at a valley mouth, approximately 100 m inland from the sea
ARN	No	NA	221 ± 1	Located on the ridge summit, out of the canopy on a small plateau
ARP	No	NA	263 ± 1	Located on the ridge summit, out of the canopy, on the summit of a small hillock. Rocky outcrops to the north-east
ARQ	No	NA	213 ± 1	Located on the north-east facing slope, out of the canopy

The heights included in the canopy description are the height of the tree with the greatest diameter at breast height recorded at the survey plot closest to each site

speeds from the north to east, and a well-defined diurnal cycle was established in the potential temperature time series. These periods were interspersed with two large cyclonic systems and a series of fronts. The cyclonic systems coincided with strong south-westerlies and a breakdown of the diurnal cycle established during the anticyclonic periods.

In order to compare the field observations with theory developed from 2-D neutral flow over forested ridges we concentrate on periods when the synoptic flow is across the ridge.

Cross-ridge flows were defined when the angle of the synoptic flow, α, is $50° < \alpha < 90°$ (henceforth, north-easterlies) and $240° < \alpha < 260°$ (henceforth, south-westerlies). The south-westerly cases based on wind direction at AWS ARP amounted to 50 h of data. North-easterlies were determined when both AWS ARP and the top sonic anemometer on T3 recorded wind directions between $\alpha = 50°$ and $\alpha = 90°$. This amounted to 15 h of data. Data from both AWS ARP and tower T3 are used to identify north-easterlies and so rule out any cases of south-westerly flow separation. The 40° window for north-easterlies is used to allow a large enough sample.

To restrict the comparison to near-neutral conditions the data are also filter based on h/L calculated at the top of tower T1 (the most exposed site), where L is the Obukhov length given by

$$L = \frac{(-\overline{u'w'})^{3/2}\theta}{\kappa g \overline{w'T'}}, \tag{1}$$

where $\overline{u'w'}$ is the momentum flux, $\overline{w'T'}$ is the kinematic heat flux, θ is the absolute potential air temperature (K), $g = 9.81\,\mathrm{m\,s^{-2}}$ is the acceleration due to gravity, and $\kappa = 0.4$ is the von Karman constant. Following Dupont and Patton (2012), we restrict the data to cases where $-0.01 \leq h/L < 0.02$ (near neutral) and $0.02 \leq z/L < 0.6$ (transition to stable). In their comparison of data over a flat orchard site during the CHATS experiment Dupont and Patton (2012) observed similar features of the flow structure in these two regimes. Limiting to near-neutral cases only would result in a rather small sample size. These regimes occurred mostly during windy and/or cloudy periods with low radiative forcing, or around the evening and morning transitions when the sensible heat flux is small. The south-westerly cases in particular are associated with stronger winds and a weak diurnal cycle of temperature. The north-easterly cases associated with high pressure are generally weaker winds and a stronger diurnal cycle so the selected cases occur around the evening and morning transitions.

3 Flow Structure and Flow Separation

Figure 3a–f shows 15-min averaged tower data for all times when the synoptic flow was south-westerly with Fig. 3a–c showing velocity profiles for each tower. The coloured circles show data from the sonic anemometers (coloured according to wind direction) and the black crosses are data from the cup anemometers. The interquartile ranges (25th–75th percentile) of the 15-min mean wind-speed data for all south-westerly periods are shown as horizontal bars. Figure 3d–f shows vertical momentum-flux profiles for each tower, where again the sonic anemometer data are coloured according to wind direction and interquartile ranges are shown. Figure 4 shows wind roses of 15-min averaged wind data for the same period for the AWS (top panel) and towers (bottom panel). The AWS cup anemometers are subject to a $0.78\,\mathrm{m\,s^{-1}}$ stalling threshold, and so wind-speed data $<1\,\mathrm{m\,s^{-1}}$ (coloured red) should be treated with caution. The sonic anemometers do not have a stalling threshold so low wind-speed data from the towers can be treated normally. Similar plots for cases when the synoptic flow was north-easterly are shown in Figs. 5 and 6.

For south-westerly flow (Figs. 3a–c, 4) the observations show strong evidence of flow separation, with the flow at tower T3 on the lee slope being predominantly north-easterly or easterly. Tower T2 on the top of the ridge appears to be close to the separation point with reversed, easterly flow deep within the canopy, but with south-westerly flow near canopy top. The AWS wind data in Fig. 4 support this conclusion, with flow from the north-east to south-east over the lee slope (AWS ARG, ARF and ARH), and also at the AWS site near the
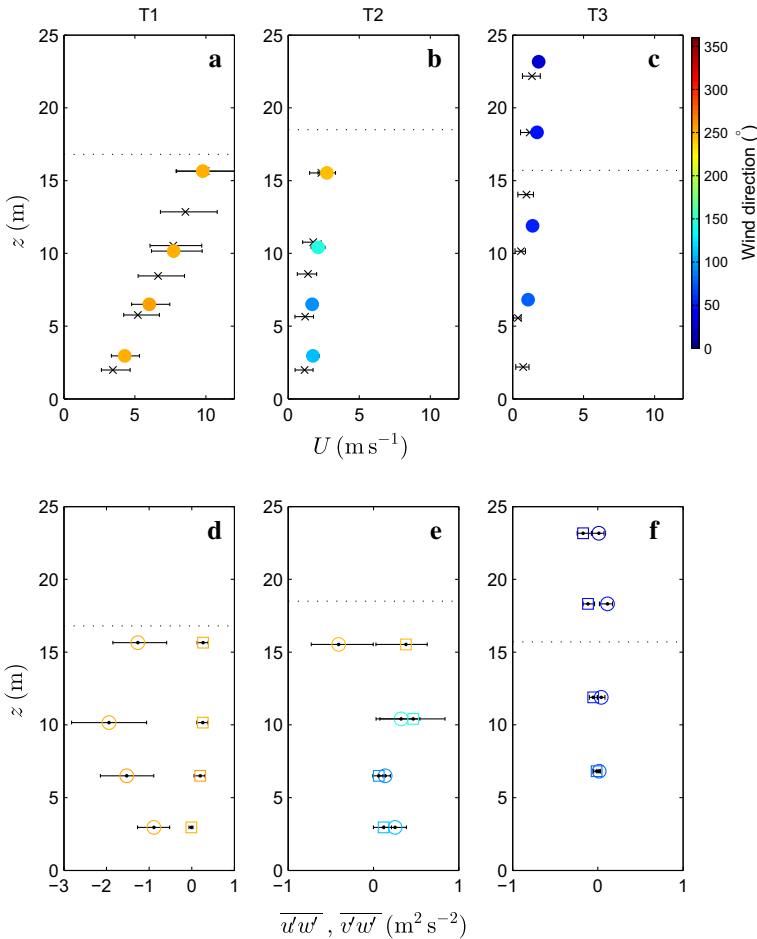
Fig. 3 a–c Wind-speed profiles for each tower during south-westerly flow. Cup anemometer data are indicated by *black crosses* with sonic anemometer data indicated by *coloured circles*, coloured according to mean wind direction. The *error bars* show the interquartile range of the 15-min mean wind-speed data. Canopy height is indicated by a *dashed line*. **d–f** Vertical momentum-flux profiles $\overline{u'w'}$ (*circles*) and $\overline{v'w'}$ (*squares*) for each tower during south-westerly flow, data coloured according to mean wind direction. Interquartile ranges of the 15-min mean momentum fluxes are shown

summit (ARN). This suggests a large region of flow separation covering most of the lee slope where there is significant forest cover. Note that within the canopy over the lee slope wind speeds are very low, almost exclusively $<1\,\mathrm{m\,s^{-1}}$. Flow separation along the ridge crest is less apparent outside the forested region, with AWS ARQ still showing broadly westerly flow, although the flow appears to be more north-westerly than south-westerly perhaps indicating the commencement of partial flow separation. The AWS ARN site, which is on clear ground, but with trees to both the south-west and north-east, shows a reversal of winds. The east slope of the ridge is sufficiently steep that flow separation might occur even in the absence of the canopy, however it seems unlikely that this would happen at AWS ARN. Interestingly there is considerable variability in wind direction over the upwind slope as well, with AWS ARA, ARB and ARC exhibiting either north-westerly or south-easterly flow.
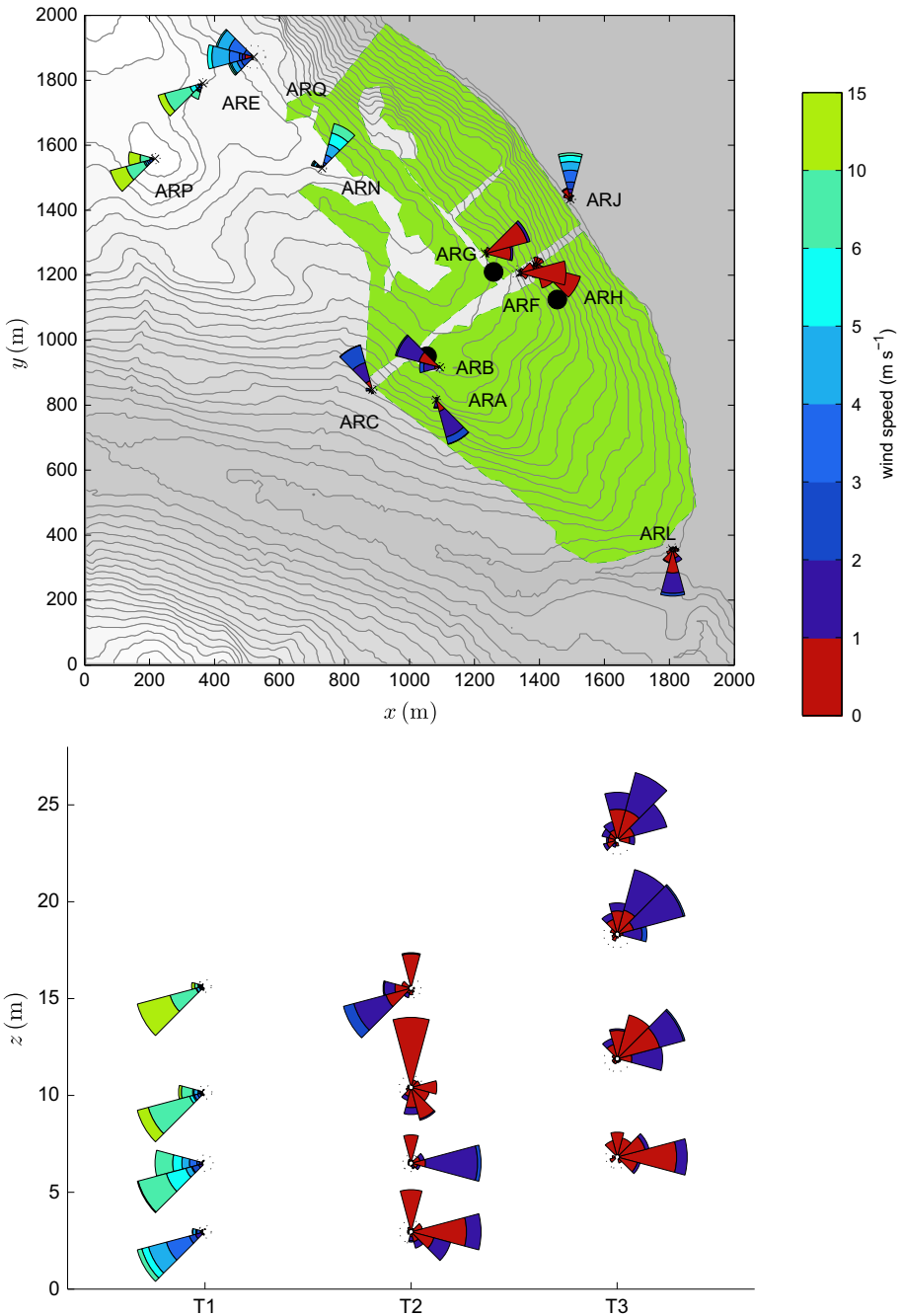
Fig. 4 15-min averaged wind data from the AWS and sonic anemometers for all times when the synoptic flow was south-westerly showing *top*: frequency distribution wind roses for wind direction, coloured according to wind speed in m s^{-1} for each AWS. *Dashed radius* indicates a frequency of 5 %. Wind roses plotted on a contour map of field site, terrain contours plotted at 10-m intervals, *shaded green marks* the forest, *black dots* mark tower locations. *Bottom* Frequency distribution plots for wind direction, coloured according to wind speed in m s^{-1} for each tower
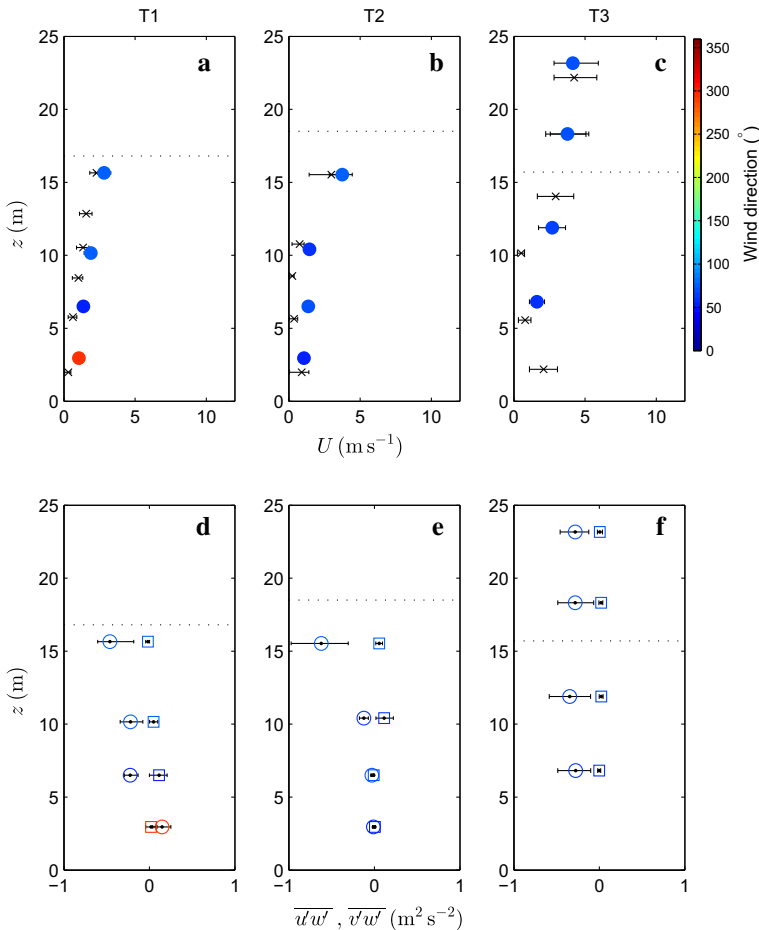
Fig. 5 As Fig. 3, but for north-easterly cases

In south-westerly flow the stronger winds at tower T1 lead to enhanced shear and a larger along-stream momentum flux, $\overline{u'w'}$ compared to the other two towers. The relatively exposed site implies that the wind shear exists right down to the surface, and that the flow cannot be considered as a pure canopy flow. The uniform wind direction implies that the cross-stream momentum flux, $\overline{v'w'}$ is much smaller. The large negative values of $\overline{u'w'}$ at the top of tower T2 (Fig. 3e) indicate a downward flux of momentum as faster moving air above the canopy is drawn down into the canopy. However, further down in the canopy $\overline{u'w'}$ is positive indicating that momentum in the along-flow direction in local streamline coordinates is transported upwards. This is somewhat counter-intuitive at first glance, but can be explained by the directional shear with height caused by the region of flow separation. This results in du/dz in streamwise coordinates being small or negative throughout much of the canopy, although the wind speed increases with height. Alongside the positive $\overline{u'w'}$, larger values of $\overline{v'w'}$, similar in magnitude to $\overline{u'w'}$, are observed, which is again consistent with directional shear being important. At tower T3 the region of separated flow appears to extend above the tower, and inside the separation region winds are very light with little variation in wind speed or
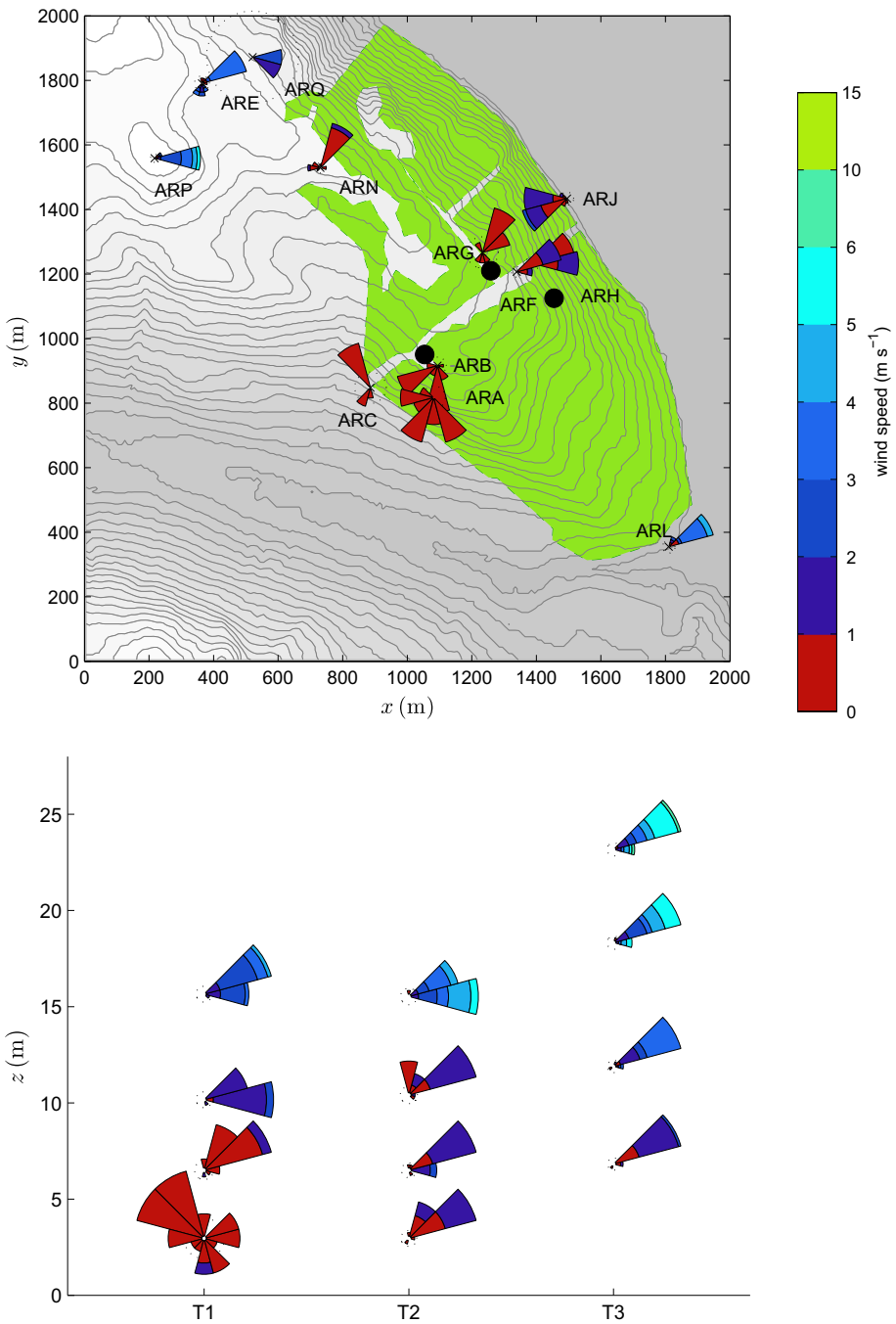
Fig. 6 As Fig. 4, but for north-easterly cases

direction with height, consistent with the small and almost constant momentum flux. Since the change in wind speed is very small, the directional shear that is present gives rise to the small positive $\overline{u'w'}$ values at tower T3.

For north-easterly flow (Figs. 5a–c, 6) wind speeds are lower than for the south-westerly cases. Consequently the flow patterns over the ridge are less defined, with much of the AWS data showing wind speeds below the $1\,\mathrm{m\,s^{-1}}$ threshold. The upwind profile at tower T3 shows much stronger winds than in south-westerly flow, even though synoptic winds are lighter. The profile above the canopy also appears closer to logarithmic in character than the south-westerly flow case where tower T3 was in the separation region; this is consistent with the nearly constant profile of $\overline{u'w'}$ and negligible $\overline{v'w'}$. For this north-easterly case there is less evidence of flow separation from the tower data over the summit and in the lee. The flow at tower T2 remains north-easterly, and at tower T1 the flow is also north-easterly except at the lowest measurement height. At this height (2.96 m) the flow is very variable in direction, but having a more westerly component. The AWS data in Fig. 6 do however provide further evidence of flow separation, with flow at sites on the windward slope being predominantly north-easterly, while over the lee slope the winds are again very light and variable with flow broadly south-westerly. The weaker and shallower flow separation seen in this case is likely to be explained by the less inclined lee slope and also the fact that tower T1 is closer to the summit of the ridge than is tower T3. As in the south-westerly case there is no strong evidence of flow separation on the transect outside the forest canopy. The AWS ARJ site, at the upwind foot of the ridge, does show a reversal in the flow with consistently westerly or south-westerly winds. This is a recurring feature of the easterly flow over this ridge and is attributed to the blocking of the low-level flow by the steeply rising land and the forest edge. At tower T1, despite the tower being mostly outside the separation region, the wind speeds decrease relatively slowly with height in the canopy, and as a result the momentum-flux values also only decay slowly with height (Fig. 5a). At the lowest point on tower T3 there is evidence of a sub-canopy jet near the ground due to the lower canopy density in the trunk space compared to higher up in the canopy. This feature is present at tower T3 in the south-westerly case as well, but is less distinct due to the generally weaker flow in the separation region. For north-easterly flow there is also some evidence of a sub-canopy jet at tower T2, which is not present in the south-westerly cases. This is due to differences in the canopy cover, with the canopy to the west of tower T2 being much denser Sitka spruce, with the trees to the east consisting of a mix of Sitka spruce and hybrid larch with a much more pronounced trunk space.

One further noticeable feature of the wind profiles in Fig. 3a–c is the much larger variability in 15-min mean wind speeds on the upwind slope, evident from the wider interquartile spread. One would expect a larger range of wind speeds at tower T1 because the mean wind speed is higher. One normalized measure of the variability is the interquartile range divided by the mean wind speed (i.e. the width of the error bars divided by the mean values in the figure). At tower T1 this gives values of 0.78–0.82, but in comparison at towers T2 and T3 values are smaller, in the range of 0.44–0.51 and 0.39–0.57 respectively. Wind speeds are often assumed to follow a Weibull distribution (e.g. Justus et al. 1976, and many subsequent studies) with a shape parameter k close to 2. Assuming this distribution, then the normalized interquartile range can be calculated as approximately 0.72. This suggests that winds on the upwind slope are slightly more variable than might be expected, while those over the summit and in the lee demonstrate significantly less variability. The north-easterly cases show a similar pattern of variability in wind speeds as occurs in the south-westerly cases, with much higher variability at the upwind tower T3 (0.67–1.08) compared to tower T2 at the summit (0.36–0.58) and tower T1 on the lee slope (0.35–0.43). This therefore seems to be a robust feature of these canopy flows.
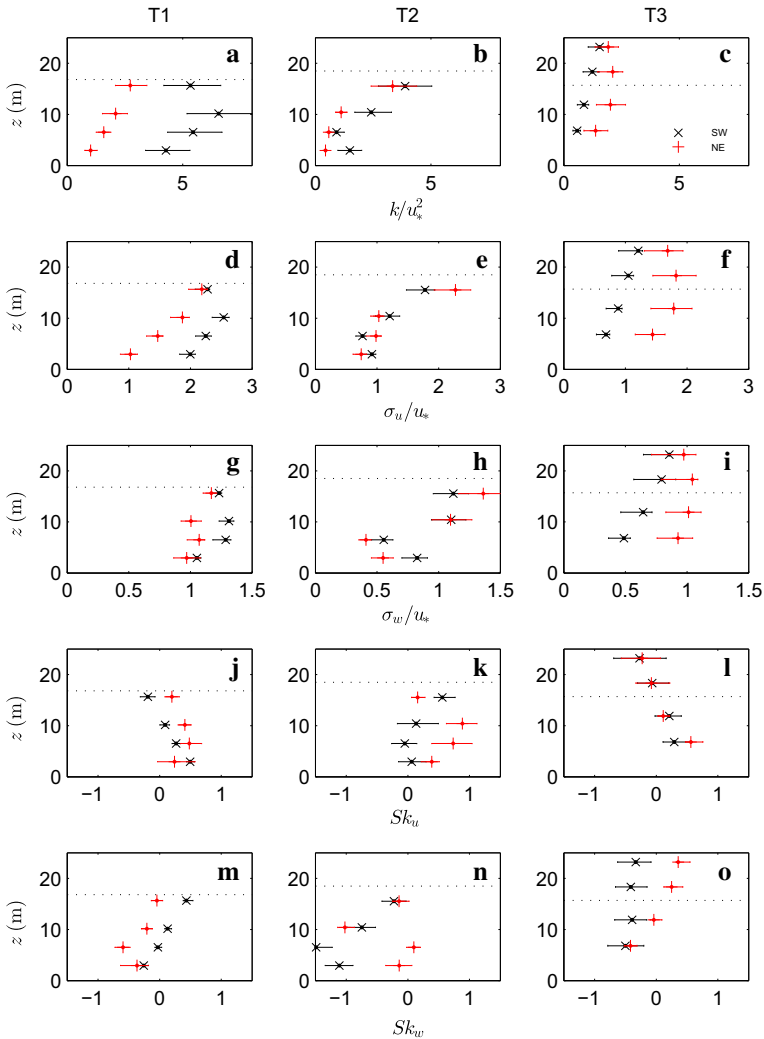
Fig. 7 Profiles of **a**–**c** turbulent kinetic energy k normalized by the friction velocity u_* squared, **d**–**f** horizontal variance normalized by the friction velocity, **g**–**i** vertical velocity variance normalized by the friction velocity, **j**–**l** horizontal velocity skewness Sk_u and **m**–**o** vertical velocity skewness Sk_w. Profiles are plotted for both south-westerly (*times*) and north-easterly (*plus*) cases at each tower. For each plot the *error bars* show the interquartile range of the 15-min averaged data

4 Profiles of Turbulence Statistics

Here, we present profiles of various turbulence statistics calculated from the sonic anemome-ter data at the three tower sites over the hill. Figure 7a–c shows profiles of turbulent kinetic energy (TKE, k) normalized by the friction velocity squared ($u_*^2 = |\overline{u'w'}|$) calculated at the top of tower T1. This is used as a reference since it is relatively exposed and gives an indication of the overall flow at a given time. Similarly Fig. 7 presents profiles of both (d–f) horizontal velocity variance (σ_u) and (g–i) vertical velocity variance (σ_w) normalized by u_* at the top

of tower T1. Using a single value of u_* allows the relative magnitude of k, σ_u and σ_w at the different towers to be assessed. It is immediately obvious that tower T1 exhibits the highest levels of turbulent kinetic energy and velocity variances, particularly in south-westerly flows. Given the relatively exposed location of tower T1 this is perhaps not surprising, since in a north-easterly flow, where tower T1 is slightly more sheltered, turbulence levels are lower. At tower T3 turbulence levels are generally lower than at tower T1, possibly due to the less exposed site, although again there is evidence of higher turbulent kinetic energy and velocity variance levels when the flow is from the north-east compared to the south-west. It is interesting to note that increased variability in the normalized 15-min mean wind at the upwind tower (Figs. 3, 5) corresponds to increased normalized turbulence levels (the mean of the 15-min TKE values). At tower T2 near the summit there is less difference in the magnitude of the turbulence levels between the two wind directions, especially at the top of the tower. What is obvious is a more rapid increase in k, σ_u and σ_w in the upper canopy compared to that at towers T1 and T3, probably related to the increased wind shear due to changes in both wind speed and direction with height. Profiles of the vertical velocity variance, σ_w/u_*, show typically smaller values than the corresponding horizontal velocity variances, with values at and above canopy top around $\sigma_u/u_* = 1.5 - 2.5$ and $\sigma_w/u_* = 1 - 1.5$.

Profiles of horizontal and vertical skewness are given in Fig. 7j–o where the skewness is given by $Sk_\chi = \overline{\chi'^3}/(\overline{\chi'^2})^{3/2}$ and χ is either the horizontal velocity component u or the vertical velocity component w. In contrast to the TKE and intensity profiles, towers T1 and T3 show similar profiles of skewness in both upwind and downwind cases. For both towers the skewness is relatively small at and above canopy top, but increases deeper into the canopy, with $Sk_u \approx 0.5$ and $Sk_w \approx -0.5$ near the ground. In contrast, bigger variations in skewness are seen between cases at tower T2. For south-westerly flow Sk_u remains small throughout the profile, with the largest values being near canopy top. In this case Sk_w is small at canopy top, but with large values of about -1 within the canopy. It is possible that this very different pattern of skewness is related to the strong directional shear seen at tower T2 for south-westerly cases where the tower is located close to the separation point of the flow. In contrast, for north-easterly flow the profiles of Sk_u are more typical, with small values at canopy top and larger values within the canopy. Sk_w however shows a peak at about 10 m (below canopy top), with values deeper in the canopy dropping close to zero again. Large changes in wind direction with height are not present at tower T2 in the north-easterly cases, however $\overline{v'w'}$ is comparable to $\overline{u'w'}$ at this height suggesting that the flow is not representative of flow over an idealized homogeneous canopy.

5 Discussion

5.1 Comparison with Idealized Models of Flow over a Forested Hill

From previous theoretical studies (e.g. Finnigan and Belcher 2004), numerical simulations (e.g. Ross and Vosper 2005) and laboratory experiments (such as Finnigan and Brunet 1995; Poggi and Katul 2007b) we have an idealized conceptual picture of flow over a two-dimensional forested ridge. The key features of this conceptual picture are seen in the field observations presented here. The ridge has slopes >0.1, and so based on Ross and Vosper (2005) we might expect flow separation. This is indeed observed, both at the towers and at the AWS. As would be expected flow separation appears to be stronger for south-westerly cases where the lee slope is steeper. Unlike the simple two-dimensional model, flow is not simply reversed over the lee slope, and there may be significant along-slope components to

the flow in these flow separation regions (e.g. at AWS ARA, ARB and ARC in Fig. 6). Both the three-dimensional nature of the terrain and the heterogeneous nature of the canopy appear to be important in determining the exact nature of the separated flow.

In previous idealized studies differences in the induced flow within and above the canopy lead to changes in the shear layer at canopy top across the hill. Over the upwind slope the shear is reduced since there is relatively little acceleration of the flow above the canopy, but there is induced upslope flow within the canopy. Near the summit the above-canopy flow accelerates to its maximum speed, while the in-canopy flow decelerates, leading to an increase in the shear layer and a sharp inflection point in the velocity profile. Over the lee slope the development of a region of flow separation leads to low wind speeds and a reversed flow direction in the canopy. Again we also see these features qualitatively in the field observations presented here (e.g. Figs. 3, 5). For the south-westerly case this is enhanced by the fact that tower T1 is at a relatively exposed site and so the flow is not a pure canopy flow. Near the summit at tower T2 we do see a large increase in the momentum flux and some evidence of the inflection point in the velocity profile, however to really confirm this would require observations further above the canopy. As might be expected, the reduced shear over the upwind slope leads to a reduction in the generated turbulent mixing at canopy top in this region, although the fact that there is a mean flow component into the canopy implies that turbulence levels in the upper canopy can actually increase due to vertical advection of more turbulent air from above. There is some evidence of this at towers T1 (for south-westerly flow) and T3 (for north-easterly flow) in both the momentum-flux profiles (Figs. 3, 5) and the TKE profiles (Fig. 7).

For south-westerly flow the tower on the lee slope (T3) shows evidence of flow separation extending well above the canopy top. Since this slope is significantly steeper than the critical slope for flow separation extending above the canopy (see Ross and Vosper 2005) this is not too surprising. It is interesting that we do not see the same features at tower T1 for north-easterly flow, even though the western slope is still relatively steep, although less steep than the eastern slope. The differences in the site may well play a role here, with tower T1 more exposed with a relatively large clearing to the west. The profiles of $\overline{u'w'}$ in Fig. 5 suggest there is significant mixing of momentum down into the canopy, and this is supported by the wind-speed profile that shows little sign of a strong inflection point near canopy top. Miller et al. (1991) and Belcher et al. (2003) have shown that, over flat ground, the mean wind speed rapidly increases as the flow exits the canopy, in response to the removal of the drag force associated with the canopy, and that there is a downward motion into the clearing to conserve mass. With its location at a distance of approximately h from the forest edge, tower T1 is very likely to be affected by these features in the north-easterly flow. As shown by Ross and Baker (2013) in their idealized model study, the flow over complex terrain with a heterogeneous canopy cover is driven by a combination of canopy-edge induced and terrain-induced pressure perturbations. Relatively localized canopy-edge effects dominate near to the canopy edge, while elsewhere terrain effects dominate. In their simulations Ross and Baker (2013) observed that flow separation was primarily constrained to within the canopy over moderate slopes, only extending a short distance beyond the edge of the canopy over the lee slope. This is consistent with the shallow separation observed here at tower T1.

The impact of forest edges and clearings can also be used to explain the south-easterly winds found at AWS ARA during south-westerly flow (Fig. 4). The theoretical model of Belcher et al. (2003) predicts an adverse pressure gradient upwind of a clearing-to-canopy transition, which acts to decelerate the flow as this approaches the forest edge. In three dimensions this deceleration may lead to deflection of the flow along the canopy edge (as seen at AWS ARA, ARB and ARC), or even to flow reversal (e.g. AWS ARJ). Similar flow

separation at the upwind edge of the canopy is seen in the LES of Cassiani et al. (2008) over flat ground and also at the upwind canopy edge on the upwind slope in the idealized 2-D numerical simulations of Ross and Baker (2013).

5.2 Comparison of Turbulence Statistics with Idealized Models

The profiles of turbulent statistics presented in Sect. 4 are broadly consistent with previous observations over flat, homogeneous canopies, as summarized for example in Raupach et al. (1996) who presented data from a number of different experiments over very different (but homogeneous) canopies. Few of the idealized studies over hills (either experimental or numerical) include turbulent statistics, although there are wind-tunnel observations presented in Finnigan and Brunet (1995). Dupont et al. (2008) largely reproduced these observations in their LES study, including additional observations unpublished in the original paper of Finnigan and Brunet (1995). Again these profiles over an idealized ridge are largely consistent with the field observations presented here. Below we highlight the key differences.

As in Finnigan and Brunet (1995) and Dupont et al. (2008), higher values of σ_u/u_* and σ_w/u_* are observed in the lower canopy at the upwind tower (T1 for south-westerly flow and T3 for north-easterly flow). This is likely to be due to the mean flow into the canopy leading to the advection of turbulence from the upper canopy, and is in line with the observed increase in TKE at these locations. Low values of σ_u/u_* and σ_w/u_* are observed above the canopy at tower T3 in south-westerly winds, probably because tower T3 is entirely within the separation region and subject to weak flow and low shear even above the canopy. The only point at tower T2 that appears to deviate from previous results over flat ground and from the wind-tunnel data is the lowest instrument level in south-westerly winds, which shows larger values of σ_w/u_* than expected (about 0.8), which are also significantly larger than at the height above. At this lowest height slightly elevated values of k/u_*^2 are also observed, along with positive momentum fluxes, larger in magnitude than at the height above. There is relatively little evidence of trunk-space flow in these conditions (thick Sitka spruce to the west of the tower), and so the increased turbulence is probably related to the strong directional shear and is a feature of the three-dimensional flow in this non-idealized situation.

In Finnigan and Brunet (1995) and Dupont et al. (2008) the skewness changes relatively little over most of the hill, with small values of both Sk_u and Sk_v aloft and Sk_u increasing to 1 to 1.5 in the canopy and Sk_w decreasing to -1 to -1.5. These are slightly higher in magnitude than many of the profiles presented in Raupach et al. (1996) for canopies on flat ground and the values do not decrease at levels lower down in the canopy. This is probably a reflection of the modelled canopy in the wind tunnel rather than the fact that the flow is over a ridge. Values are quite variable in the wind-tunnel data over the summit and just downwind, but there does appear to be peaks in both Sk_u and Sk_w near canopy top above the summit. In the recirculation region in the wind tunnel Sk_u takes its largest positive values and Sk_w takes its largest negative values. The variations in skewness across the hill seen in the field observations presented here are broadly consistent with those in Finnigan and Brunet (1995), although the values of the skewnesses are less than those seen in the wind-tunnel experiments. The key location where the skewness differs from the results over flat ground presented in Raupach et al. (1996) is at tower T2 in south-westerly winds where Sk_u is small throughout most of the canopy, only increasing towards canopy top. In contrast Sk_w has large negative values in the canopy (up to -1.5). So in this region close to flow separation and with strong directional shear the horizontal wind field shows relatively little skewness, while vertical motion is dominated by strong downward gusts from the upper canopy. The only other notable difference from skewness profiles over flat ground are near canopy top at tower

T3. For north-easterly cases Sk_w becomes slightly positive above the canopy, while it remains negative for south-westerly cases. In the south-westerly flow the tower is entirely within the separation region and so strong downward events dominate. In contrast, for the north-easterly cases the mean flow and other turbulent statistics profiles are similar to those for flat ground, and so this slight increase in strong upward motion events is somewhat surprising.

6 Conclusions

A unique set of airflow measurements from within and above a forest canopy in complex terrain has been presented. This dataset provides much needed information to help support and improve our current understanding and modelling of canopy flows over complex hetero-geneous terrain.

Data from across-ridge flows have been presented and have been shown, at least qualitatively, to be in agreement with predictions from idealized two-dimensional theory, numerical models and wind-tunnel experiments. In particular the occurrence of flow separation appears to be a common event in both south-westerly and north-easterly flows, although the details of the separation are very dependent on local heterogeneities in the canopy cover and the terrain. Clearings in the canopy have been seen to modify the wind profile and reduce or prevent the formation of flow separation, even at a short distance of order h into the clearing. Cases such as these have highlighted the necessity to explicitly model the canopy and to capture the canopy heterogeneity if models are to accurately predict flow patterns (including flow separation) over small-scale hills, or if comparison is to be made with observations made in clearings. The occurrence of flow separation can also have significant effects on scalar transport, as highlighted by Ross (2011) and so such details are also likely to be important in the planning and interpretation of flux measurements at sites in complex terrain.

The observed flow is strongly three dimensional with strong directional shear with height in regions of flow separation. This has a significant impact on the Reynolds stress terms $\overline{u'w'}$ and $\overline{v'w'}$ with $\overline{u'w'}$ being positive and $\overline{v'w'}$ being similar in magnitude to $\overline{u'w'}$ at a number of locations, particularly for south-westerly flows with larger-scale flow separation. This is something not seen in the many idealized two-dimensional theoretical and modelling studies and makes interpretation of the flow and direct comparison with simple theories complicated. The strong directional shear may be important for wind damage to trees and for wind energy applications since it may place additional torsional forces on the trees or wind turbines. Higher-order turbulence statistics show similarities with profiles over flat ground at some sites and for some wind directions, but there are also significant differences, again particularly around regions with strong directional shear.

In future this dataset should offer useful opportunities to test the validity of the turbulence closure schemes used in numerical models of canopy flow in complex and heterogeneous terrain. It will also be important to validate the models themselves for predicting flow in such conditions. Such validation beyond simple idealized problems is essential if these models are to be used to understand complex canopy flows and to make predictions of the impact of such flows.

References

Allen T, Brown AR (2002) Large-eddy simulation of turbulent separated flow over rough hills. Boundary-Layer Meteorol 102:177–198. doi:10.1023/A:1013155712154

Ayotte KW, Davy RJ, Coppin PA (2001) A simple temporal and spatial analysis of flow in complex terrain in the context of wind energy modelling. Boundary-Layer Meteorol 98:275–295. doi:10.1023/A:1026583021740

Baldocchi D, Falge E, Gu LH, Olson R, Hollinger D, Running S, Anthoni P, Bernhofer C, Davis K, Evans R, Fuentes J, Goldstein A, Katul G, Law B, Lee XH, Malhi Y, Meyers T, Munger W, Oechel W, Paw UKT, Pilegaard K, Schmid H, Valentini R, Verma S, Vesala T, Wilson K, Wofsy S (2001) FLUXNET: a new tool to study the temporal and spatial variability of ecosystem-scale carbon dioxide, water vapor, and energy flux densities. Bull Am Meteorol Soc 82:2415–2434. doi:10.1023/A:1002497616547

Belcher SE, Hunt JCR (1998) Turbulent flow over hills and waves. Annu Rev Fluid Mech 30:507–538. doi:10.1146/annurev.fluid.30.1.507

Belcher SE, Jerram N, Hunt JCR (2003) Adjustment of a turbulent boundary layer to a canopy of roughness elements. J Fluid Mech 488:369–398. doi:10.1017/S0022112003005019

Belcher SE, Finnigan JJ, Harman IN (2008) Flows through forest canopies in complex terrain. Ecol Appl 18:1436–1453. doi:10.1890/06-1894.1

Bradley EF (1980) An experimental study of the profiles of wind speed, shearing stress and turbulence at the crest of a large hill. Q J R Meteorol Soc 106:101–123. doi:10.1002/qj.49710644708

Brown AR, Hobson JM, Wood N (2001) Large-eddy simulation of neutral turbulent flow over rough sinusoidal ridges. Boundary-Layer Meteorol 98:411–441. doi:10.1023/A:1018703209408

Cassiani M, Katul GG, Albertson JD (2008) The effects of canopy leaf area density on airflow across forest edges: large-eddy simulation and analytical results. Boundary-Layer Meteorol 126:433–460. doi:10.1007/s10546-007-9242-1

Dupont S, Brunet Y (2008) Edge flow and canopy structure: a large-eddy simulation study. Boundary-Layer Meteorol 126:51–71. doi:10.1007/s10546-007-9216-3

Dupont S, Patton EG (2012) Influence of stability and seasonal canopy changes on micrometeorology within and above an orchard canopy: The CHATS experiment. Agric For Meteorol 157:11–29. doi:10.1016/j.agrformet.2012.01.011

Dupont S, Brunet Y, Finnigan JJ (2008) Large-eddy simulation of turbulent flow over a forested hill: validation and coherent structure identification. Q J R Meteorol Soc 134:1911–1929. doi:10.1002/qj.328

Finnigan JJ (2000) Turbulence in plant canopies. Annu Rev Fluid Mech 32:519–571. doi:10.1146/annurev.fluid.32.1.519

Finnigan JJ (2008) An introduction to flux measurements in difficult conditions. Ecol Appl 18:1340–1350. doi:10.1890/07-2105.1

Finnigan JJ, Belcher SE (2004) Flow over a hill covered with a plant canopy. Q J R Meteorol Soc 130:1–29. doi:10.1256/qj.02.177

Finnigan JJ, Brunet Y (1995) Turbulent airflow in forests on flat and hilly terrain. In: Coutts MP, Grace J (eds) Wind and trees. Cambridge University Press, Cambridge, pp 3–40

Foken T, Wichura B (1996) Tools for quality assessment of surface-based flux measurements. Agric For Meteorol 78:83–105. doi:10.1016/0168-1923(95)02248-1

Gardiner B, Blennow K, Carnus JM, Fleischer P, Ingemarson F, Landmann G, Lindner M, Marzano M, Nicoll B, Orazio C, Peyron JL, Reviron MP, Schelhaas MJ, Schuck A, Spielmann M, Usbeck T (2010) Destructive storms in European forests: past and forthcoming impacts. Final Report to European Commission DG Environment. Online. http://ec.europa.eu/environment/forests/fprotection.htm

Gardiner B, Schuck A, Schelhaas MJ, Orazio C, Blennow K, Nicoll B (eds) (2013) Living with storm damage to forests: what science can tell us 3. European Forest Institute. http://www.efi.int/files/attachments/publications/efi_wsctu_3_final_net.pdf

Hanewinkel M, Cullmann D, Schelhaas M, Nabuurs GJ, Zimmermann N (2013) Climate change may cause severe loss in the economic value of European forest land. Nat Clim Change 3:203–207. doi:10.1038/nclimate1687

Hunt JCR, Leibovich S, Richards KJ (1988) Turbulent shear flow over low hills. Q J R Meteorol Soc 114:1435–1470. doi:10.1002/qj.49711448405

Irvine MR, Gardiner BA, Hill MK (1997) The evolution of turbulence across a forest edge. Boundary-Layer Meteorol 84:467–496. doi:10.1023/A:1000453031036

Justus CG, Hargreaves WR, Yalcin A (1976) Nationwide assessment of potential output from wind-powered generators. J Appl Meteorol 15:673–678. doi:10.1175/1520-0450(1976)015<0673:NAOPOF>2.0.CO;2

Kaimal JC, Finnigan JJ (1994) Atmospheric boundary layer flows: their structure and measurements. Oxford University Press, New York 289 pp

Lee X, Finnigan J, Paw UKT (2004) Coordinate systems and flux bias error. In: Lee X, Massman W, Law B (eds) A handbook of micrometeorology: a guide for surface flux measurements. Kluwer, Dordrecht, pp 33–66

Miller DR, Lin JD, Lu ZN (1991) Air flow across an alpine forest clearing: a model and field measurements. Agric For Meteorol 56:209–225. doi:10.1016/0168-1923(91)90092-5

Morse AP, Gardiner BA, Marshall BJ (2002) Mechanisms controlling turbulence development across a forest edge. Boundary-Layer Meteorol 103:227–251. doi:10.1023/A:1014507727784

Neff DE, Meroney NR (1998) Wind-tunnel modelling of hill and vegetation influence on wind-power availability. J Wind Eng Ind Aerodyn 74:335–343. doi:10.1016/S0167-6105(98)00030-0

Patton EG, Katul GG (2009) Turbulent pressure and velocity perturbations induced by gentle hills covered with sparse and dense canopies. Boundary-Layer Meteorol 133:189–217. doi:10.1007/s10546-009-9427-x

Poggi D, Katul GG (2007a) An experimental investigation of the mean momentum budget inside dense canopies on narrow gentle hilly terrain. Agric For Meteorol 144:1–13. doi:10.1016/j.agrformet.2007.01.009

Poggi D, Katul GG (2007b) Turbulent flows on forested hilly terrain: the recirculation region. Q J R Meteorol Soc 133:1027–1039. doi:10.1002/qj.73

Quine C, Gardiner BA (2007) Understanding how the interaction of wind and trees results in windthrow, stem breakage and canopy gap formation. In: Johnson E, Miyanishi K (eds) Plant disturbance ecology: the process and the response. Academic Press, Burlington, pp 103–155

Raupach MR, Finnigan JJ, Brunet Y (1996) Coherent eddies and turbulence in vegetation canopies: the mixing length analogy. Boundary-Layer Meteorol 78:351–382. doi:10.1007/BF00120941

Romniger JT, Nepf HM (2011) Flow adjustment and interior flow associated with a rectangular porous obstruction. J Fluid Mech 680:636–659. doi:10.1017/jfm.2011.199

Ross AN (2008) Large eddy simulations of flow over forested ridges. Boundary-Layer Meteorol 128:59–76. doi:10.1007/s10546-008-9278-x

Ross AN (2011) Scalar transport over forested hills. Boundary-Layer Meteorol 141:179–199. doi:10.1007/s10546-011-9628-y

Ross AN, Baker TP (2013) Flow over partially forested ridges. Boundary-Layer Meteorol 146. doi:10.1007/s10546-012-9766-x

Ross AN, Vosper SB (2005) Neutral turbulent flow over forested hills. Q J R Meteorol Soc 131:1841–1862. doi:10.1256/qj.04.129

Ruck B, Adams E (1991) Fluid mechanical aspects of the pollutant transport to coniferous trees. Boundary-Layer Meteorol 56:163–195. doi:10.1007/BF00119966

Vosper SB, Mobbs SD, Gardiner BA (2002) Measurements of the momentum budget in flow over a hill. Q J R Meteorol Soc 128:2257–2280. doi:10.1256/qj.01.11

Webster S, Brown AR, Cameron DR, Jones CP (2003) Improvements to the representation of orography in the Met Office Unified Model. Q J R Meteorol Soc 129:1989–2010. doi:10.1256/qj.02.133

Zeri M, Rebmann C, Feigenwinter C, Sedlak P (2010) Analysis of short periods with strong and coherent CO_2 advection over a forested hill. Agric For Meteorol 150(5):674–683. doi:10.1016/j.agrformet.2009.12.003